Gold Nanoparticles

DOI: 10.1002/anie.201201283

Intrinsic Catalytic Structure of Gold Nanoparticles Supported on TiO_2**

*Yasufumi Kuwauchi, Hideto Yoshida, Tomoki Akita, Masatake Haruta, and Seiji Takeda**

It is well known that gold nanoparticles (GNPs) supported on TiO_2 act as catalysts for the oxidation of CO, even below room temperature.[1] Since bulk gold does not exhibit catalytic activity, numerous studies have focused on the structure of the Au/TiO_2 catalyst, both experimentally and theoretically.[2] To elucidate the microscopic mechanism of Au/TiO_2 catalysts, in situ observations under reaction conditions are necessary. Transmission electron microscopy (TEM) has been used to determine the structures of Au/TiO_2 catalysts in vacuum and gases.[3] However, under electron irradiation the TiO_2 supports were much more fragile than other supports such as CeO_2. The TiO_2 supports were easily damaged and their crystallinity degraded during TEM observation.[4] Also, it has recently been reported that the interface between a GNP and the TiO_2 support is structurally reorganized.[5] To deduce the intrinsic structure of the most common GNP catalyst (Au/TiO_2) without electron irradiation, systematic environmental TEM (ETEM) studies are required. Herein we report for the first time the intrinsic structure of the Au/TiO_2 catalyst under reaction conditions. We also conclude that structural reorganization is not directly correlated with the activity of Au/TiO_2 catalysts.

We studied two types of active Au/TiO_2 catalyst samples that were prepared by the deposition precipitation method and underwent different pretreatments. The mean diameters of GNPs were estimated to be (3.4 ± 0.9) nm with a Au loading of 1.2 wt% (hereafter called sample 1) and (1.9 ± 0.5) nm with a Au loading of 3.1 wt% (sample 2). No GNPs smaller than 1.9 nm were observed in sample 1. The metal time yields (MTYs) at 30 °C of samples 1 and 2 were 5.1×10^{-1} and 3.3×10^{-1} $mol_{CO}\,mol_{Au}^{-1}\,s^{-1}$, respectively. Detailed information on each sample is given in the Experimental Section and in the Supporting Information. It is noteworthy that the Au/TiO_2 samples in this study are typical nanoparticulate gold catalysts with high activity for the oxidation of CO at room temperature. Since the TiO_2 supports had different crystallinity and the size distribution of GNPs was not narrow enough, the difference in the MTYs was not unusual and within an acceptable range. For a quantitative discussion on the size effect of GNPs, well-defined surface science model catalysts having the same metal loading but different mean particle diameters are the most suitable. Fujitani et al.[2c] have recently reported that the MTY increases in inverse proportion to the second power of the mean diameter, indicating that the perimeter interfaces around GNPs are the sites for CO oxidation.

Figure 1 a,b presents images of GNPs supported on TiO_2 in sample 1 recorded in situ. In the reaction gas (1 vol% CO in air (100 Pa)), the {111} and {100} facets of the GNPs were exposed to the reaction gas, which was apparent from the lateral view (Figure 1 a). It is also evident that the bottom portion of the GNP frequently tapered toward the flat interface of the TiO_2 support. In the top view (Figure 1 b), the edges extended parallel to the ⟨110⟩ directions. Since the GNPs in Figure 1 were viewed parallel to the ⟨110⟩ zone axes, two types of mutually intersecting {111}-type lattice planes with intervals of 0.24 nm were visible. In contrast to previous studies,[5b,c] the interface between the GNP and the TiO_2 supports remained stable, without any detectable structural reorganization. Also, GNPs changed their morphology systematically depending on the environment. In vacuum and inert N_2 (100 Pa), {111} and {100} facets were observed (Figure 1 a,b). The round morphology of the GNP in O_2 likely resulted from the activation of O_2 molecules at the perimeter of the interface between the GNP and the metal oxide support.[6] Even though the atomic structures of the GNPs and their interfaces with the support were not identical in the Au/TiO_2 catalyst sample, the majority of GNPs (approximately 60%) reproduced the same facetted morphology in the reaction gas, regardless of the sequence of exchanging gases. Similar systematic changes in the morphology of GNPs in sample 2 were also observed and they are presented in the Supporting Information. Despite the fragility of TiO_2, it was confirmed that the TiO_2 supports maintained crystallinity during the morphological changes of GNPs in various gases (see also the Supporting Information).

[*] Y. Kuwauchi, Dr. H. Yoshida, Prof. S. Takeda
The Institute of Scientific and Industrial Research
Osaka University
8-1 Mihogaoka, Ibaraki, Osaka 567-0047 (Japan)
E-mail: takeda@sanken.osaka-u.ac.jp
Y. Kuwauchi
Department of Physics, Graduate School of Science
Osaka University
1-1 Machikaneyama, Toyonaka, Osaka 560-0043 (Japan)
Dr. T. Akita
Research Institute for Ubiquitous Energy Devices
National Institute of Advanced Industrial Science and Technology
1-8-31, Midorigaoka, Ikeda, Osaka 563-8577 (Japan)
Prof. M. Haruta
Department of Applied Chemistry, Graduate School of Urban Environmental Sciences, Tokyo Metropolitan University
1-1 Minami-osawa, Hachioji, Tokyo 192-0397 (Japan)

[**] This study was supported by a Grant-in-Aid for Specially Promoted Research (grant no. 19001005) from the Ministry of Education, Culture, Sports, Science and Technology (MEXT) (Japan). A part of this study was supported by the "Low-Carbon Research Network (Handai satellite)" of MEXT. We thank Dr. S. Tanaka, Dr. K. Tanaka, and Prof. M. Kohyama of AIST for their interest in this study.

Supporting information for this article is available on the WWW under http://dx.doi.org/10.1002/anie.201201283.

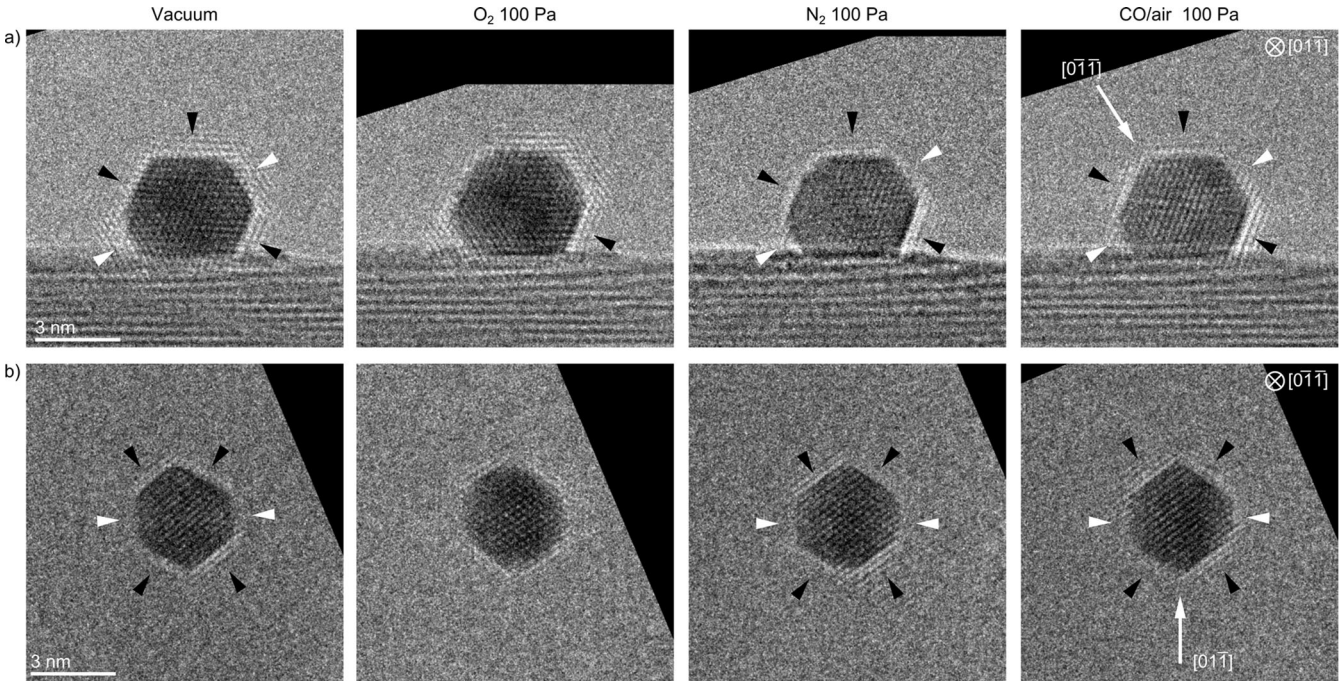

Figure 1. GNPs supported on TiO_2. a) Lateral view of a GNP and b) top view of a different GNP. The viewing directions are $[01\bar{1}]$ in (a) and $[0\bar{1}\bar{1}]$ in (b). Black and white arrow heads indicate {111}- and {100}-type facets, respectively. The environment was varied from vacuum to O_2 (100 Pa) to N_2 (100 Pa) and to 1 vol% CO in air (100 Pa). Samples underwent electron irradiation only for acquiring ETEM images with a small electron current density, $\phi = 3.0\,A\,cm^{-2}$.

Recently, significant attention has focused on the potential of in situ TEM and ETEM for studying chemical and catalytic reactions at an atomic scale.[6,7] To deduce structural information that directly correlates with catalytic activity, the effect of electron irradiation needs to be eliminated and studied systematically. Figure 2 presents typical reorganization processes of sample 1 in different environments (vacuum, O_2 (100 Pa) and 1 vol% CO in air (100 Pa)). The perimeter interface between the GNP and the TiO_2 support was gradually decorated with material coming from the support with increasing electron irradiation time, τ, independent of the environment. After decoration, the GNP was lifted, producing a pillar beneath it (Figure 2 a,c). This result was reported in previous studies of Au/TiO_2[5c] and the associated Au/MgO system.[8] Pillars and capsules were confirmed to be made up of titanium and oxygen. Electron energy loss spectroscopy (EELS) and energy-dispersive X-ray analysis (EDX) detected titanium and oxygen in pillars and capsules. Furthermore, several pillars and capsules exhibited lattice fringes that can be identified as rutile-type or anatase-type structures that were epitaxial with the support. Detailed elemental and structural analyses of pillars and capsules are described in the Supporting Information. To quantify the electron-irradiation-induced structural reorganization, several GNPs in sample 1 were observed with increasing τ, while the electron current density, ϕ, was held constant. The results were summarized as structure evolution diagrams under electron irradiation as a function of ϕ and electron dose, D, ($D = \phi\tau$) (Figure 3). Technical details for the derivation of the diagram are described in the Supporting Information. In regions of low ϕ and low D, structural reorganization was not detected within the spatial resolution available in the ETEM. The regions without structural reorganization are indicated by green in vacuum, O_2 (100 Pa), and 1 vol% CO in air (100 Pa) in Figure 3. The GNPs presented in Figure 1 a,b were within the green region in Figure 3. Additionally, the Supporting Information presents ETEM observations of sample 2 in the green region of Figure 3. With increasing τ, D increased linearly, and it went beyond the green region. For example, a permissible observation time (within the green region) for $\phi = 10.0\,A\,cm^{-2}$ in a typical high-resolution microscopy observation was limited to only a few hundred seconds. Over that time, structural reorganization occurred. Figure 3 also shows that structural reorganization is an irreversible process with increasing τ and D, meaning the structural reorganization was not directly correlated with the catalytic activity of Au/TiO_2. By extrapolating the structure at $\phi = 0$ and $D = 0$ from the structure evolution diagram, it was possible to deduce the intrinsic structure of catalysts (under no electron irradiation) under reaction conditions. We concluded that the intrinsic structures can be within the green regions in Figure 3. To our knowledge, a structure evolution diagram, especially for a heterogeneous catalyst, has not previously been derived. Similar diagrams may be helpful to deduce intrinsic structures and/or intrinsic phenomena in various chemical reactions that can be producible in TEMs and ETEMs.

Figure 4 presents the structure of a GNP that was determined under the reaction conditions in this study. The indexes of facets, edges, and viewing directions are consistent with the observations presented in Figure 1. Consistent with the number density of CO and O_2 gas molecules in the

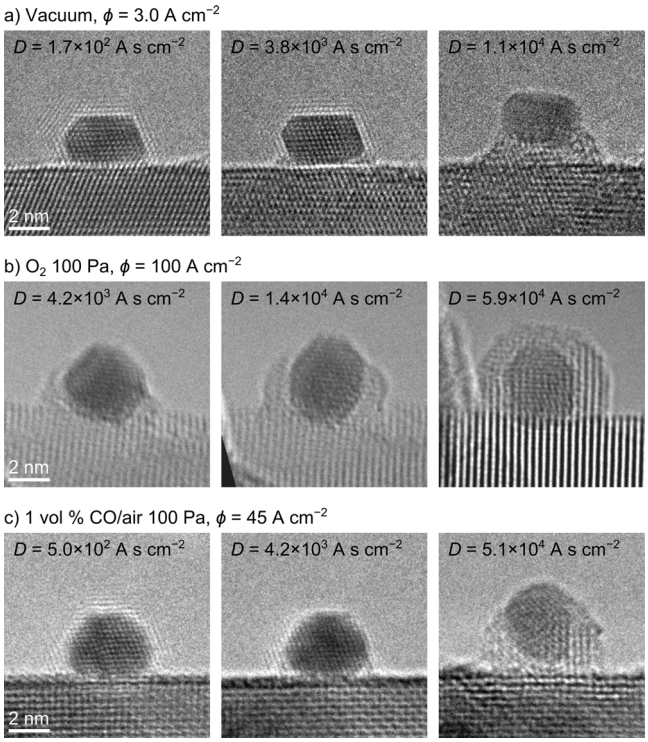

Figure 2. Typical structural reorganization processes in Au/TiO_2 under electron irradiation. a) In vacuum. Electron current density, $\phi = 3.0\,A\,cm^{-2}$. A perimeter interface was decorated with support material after continuous electron irradiation for approximately 1000 s and a pillar formed. b) In O_2 (100 Pa). $\phi = 100\,A\,cm^{-2}$. At this high current density, GNPs were occasionally encapsulated without formation of a pillar. c) In 1 vol% CO in air (100 Pa). $\phi = 45\,A\,cm^{-2}$. A GNP was decorated with support material after continuous observation for approximately 100 s and a pillar formed. The electron dose, *D*, is presented in each image.

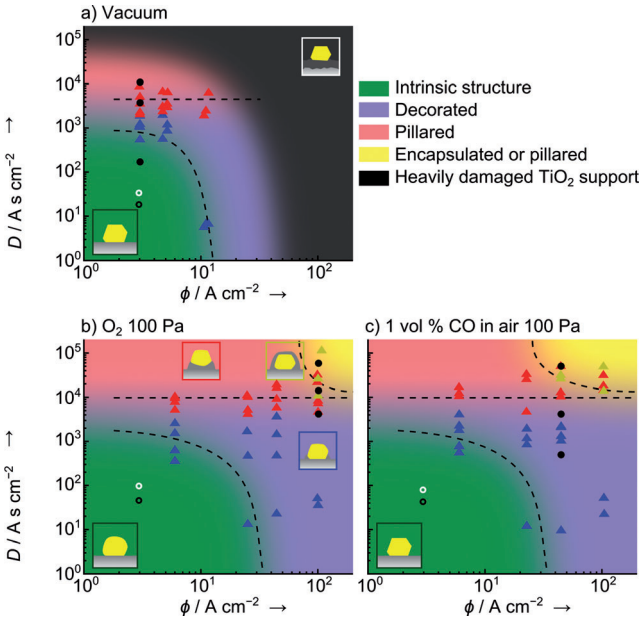

Figure 3. Structure evolution diagrams of Au/TiO_2 catalysts under electron irradiation as a function of electron current density, ϕ, and dose, *D*, in a) vacuum, b) O_2 (100 Pa), and c) 1 vol% CO in air (100 Pa) at room temperature. The intrinsic structures were observed in the green regions, while GNPs with decorations and pillars were observed in the blue and red regions, respectively. In the yellow regions, either GNPs with pillars or encapsulated GNPs were observed. A blue, red, or yellow triangle indicates the *D* at which decoration, pillar, or encapsulation around a GNP was first detected at a given current density. In vacuum, TiO_2 supports were heavily damaged, as shown in the black region in (a). The dose for acquiring an ETEM image in Figure 1a, Figure 1b, and Figure 2 at the smallest current density ($3.0\,A\,cm^{-2}$) in the present study is marked by open black, open white, and filled black circles, respectively (see the note in the Supporting Information.)

reaction gas, only one CO gas molecule and one O_2 gas molecule are depicted in the instantaneous view in Figure 4, while CO and O_2 molecules collide with a surface Au atom at significant rates of approximately 2×10^3 and $4\times10^4\,s^{-1}$, respectively. It is widely accepted that CO molecules are preferentially adsorbed to edges and steps on the surface of GNPs, rather than to the facets (Figure 4).[9] Recent studies have suggested that the catalytically active sites are located at or near the perimeter interface.[2c,d,6,10] It is noteworthy that GNPs exhibit catalytic activity when they are supported on various metal oxides, such as TiO_2 and CeO_2, which have different crystal structures. Therefore, the activity of GNP catalysts most likely originates from the structure of GNPs at perimeter interfaces commonly formed on any relevant metal oxides, especially at edges parallel to the ⟨110⟩ directions, as presented in this study (Figure 4). Despite extensive efforts directed toward Au/TiO_2 catalysis, previous in situ observations of GNPs in catalysis are mutually conflicting; that is, there are round,[5a] pillared,[5c] and unstable[5d] structures. This conflict in pioneering works was possibly due to a poorly defined environment in ETEM instruments and much less care being taken about the effect of electron irradiation. Therefore, the observation of GNPs in Au/TiO_2 catalyst in the reaction environment in this study has advanced the operando

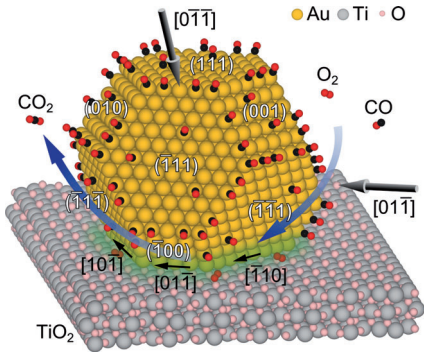

Figure 4. Instantaneous view of a GNP under reaction conditions (in 1 vol% CO in air (100 Pa) at room temperature). A GNP, bounded by {111} and {100} facets, has a polygonal interface with the TiO_2 support. The edges of the polygonal, or perimeter interface, are parallel to the ⟨110⟩ directions. Possible catalytically active sites are highlighted in green. The viewing directions in Figure 1 are indicated by solid arrows. In the lateral view (Figure 1a), the segment of the perimeter interface along [01$\bar{1}$] were observed end-on. In the top view (Figure 1b), the facets on ($\bar{1}$00), ($\bar{1}\bar{1}$1), and ($\bar{1}$1$\bar{1}$) were parallel to the viewing direction; therefore, the segments of the perimeter interface parallel to the [01$\bar{1}$], [10$\bar{1}$] and [$\bar{1}$10] directions were directly observed at the ends of the corresponding facets.

structural analysis of the catalysts. Direct comparison of catalytic activity and the density of the atomic structure of active sites will make it possible to infer the atomistic view of the origin of the GNP catalysts. This atomic structure analysis remains for future studies.

Oxygen in the metal oxide support may be desorbed by electron irradiation during ETEM observation. The average oxygen loss from the TiO_2 support was quantified using EELS[11] combined with point defects rate theory[12] (see the Supporting Information). Oxygen loss was detected in vacuum, but it was fully compensated in O_2 (100 Pa) and 1 vol% CO in air (100 Pa) (see the Supporting Information). Structural reorganization in the Au/TiO_2 catalyst, especially in these environments that included oxygen (Figure 2b,c and Figure 3b,c), was not the result of loss of oxygen. Structural reorganization was never observed in another GNP catalyst, Au/CeO_2.[6] It is well known that CeO_2 is an efficient oxygen-absorbing/releasing material,[13] suggesting that the framework of Ce atoms with valence fluctuations likely remained stable during the desorption and absorption of oxygen. In contrast, a family of titanium oxides, such as TiO_2-II and TiO,[4c] are induced by intense electron irradiation, especially on the surface of a thin Ti-O foil. Because of this, it is likely that the surface of the TiO_2 support is structurally and chemically inhomogeneous at electron irradiation conditions especially beyond the regions in green in Figure 3. In the unstable surface layer, Ti atoms may migrate randomly with associated oxygen atoms to form decorations and other reorganized structures at the perimeter interface.

In summary, systematic ETEM observations were used to derive the intrinsic structure of GNPs approximately ranging in size from 2 to 5 nm in the typical and most studied Au/TiO_2 catalysts under reaction conditions. This study provided experimental evidence of the structure of GNPs, including the perimeter interface with a TiO_2 support within the spatial resolution available in ETEM. Further studies are possible through in situ ETEM observations to infer what factors lead to the high activity at an atomic scale and to elucidate the catalytic mechanism of GNPs supported on oxides from the viewpoints of both chemistry and physics.

Experimental Section

Two types of Au/TiO_2 catalyst samples (samples 1 and 2) were prepared by the deposition precipitation method.[14] For sample 1, P-25 (Degussa) powder, which is a mixture of rutile and anatase, was used as the support. The nominal and actual Au contents of sample 1 were 3 wt% and 1.2 wt%, respectively. Sample 1 was calcined in air at 400 °C for 4 h. For sample 2, hydrothermally synthesized TiO_2 was used as the support. The nominal and actual Au contents of sample 2 were 5 wt% and 3.1 wt%, respectively. Sample 2 was calcined in H_2/N_2 stream at 300 °C for 2 h. The mean diameters of the GNPs were estimated by high-angle annular dark-field scanning transmission electron microscopy to be (3.4 ± 0.9) nm for sample 1 and (1.9 ± 0.5) nm for sample 2. The activity of the Au/TiO_2 catalysts was measured using a fixed-bed flow reactor by passing 1 vol% CO in air at a space velocity of 20000 $mL\,h^{-1}\,g_{cat}^{-1}$. The conversion of CO to CO_2 by sample 1 and sample 2 reached 50% at −27 °C and −63 °C, respectively. The MTYs at 30 °C of samples 1 and 2 were estimated to be 5.1×10^{-1} and 3.3×10^{-1} $mol_{CO}\,mol_{Au}^{-1}\,s^{-1}$, respectively. See also the Supporting Information for details about the samples.

ETEM observations of sample 1 were performed using a FEI Tecnai F20 transmission electron microscope equipped with a specially designed environmental cell. The ETEM accelerating voltage was 200 kV. The nominal point resolution was 0.24 nm and the information limit was better than 0.20 nm at 100 Pa of N_2 gas. Gaseous 1 vol% CO in air, O_2, and N_2 were introduced into the environmental cell and the catalyst samples were observed at room temperature. Residual gases in the ETEM were measured using a quadrupole mass spectrometer. The total residual gas pressure was approximately 6.5×10^{-2} Pa. The partial pressures of the constituent gases were: 5.9×10^{-2} Pa H_2O, 0.3×10^{-2} Pa N_2, 0.2×10^{-2} Pa O_2, and 0.1×10^{-2} Pa CO_2. ETEM observations of sample 2 were performed using an FEI Titan ETEM equipped with a specially designed environmental cell. Details of ETEM observations of sample 2 are fully described in the Supporting Information. An additional note on the ETEM observation is described in the Supporting Information. Elemental analyses of the catalyst samples were performed before and after ETEM observations using electron energy loss spectroscopy (EELS) and energy-dispersive X-ray analysis (EDX) associated with an analytical TEM operated at 200 kV.

Received: February 15, 2012
Published online: June 22, 2012

Keywords: CO oxidation · gold · heterogeneous catalysis · nanoparticles · TiO_2

[1] M. Haruta, *Catal. Today* **1997**, *36*, 153 – 166.
[2] a) G. C. Bond, D. T. Thompson, *Gold Bull.* **2000**, *33*, 41 – 51; b) M. S. Chen, D. W. Goodman, *Acc. Chem. Res.* **2006**, *39*, 739 – 746; c) T. Fujitani, I. Nakamura, *Angew. Chem.* **2011**, *123*, 10326 – 10329; *Angew. Chem. Int. Ed.* **2011**, *50*, 10144 – 10147; d) I. X. Green, W. Tang, M. Neurock, J. T. J. Yates, *Science* **2011**, *333*, 736 – 739; e) M. Haruta, *CATTECH* **2002**, *6*, 102 – 115.
[3] a) T. Akita, M. Okumura, K. Tanaka, M. Kohyama, M. Haruta, *J. Mater. Sci.* **2005**, *40*, 3101 – 3106; b) T. Akita, M. Okumura, K. Tanaka, M. Kohyama, M. Haruta, *Catal. Today* **2006**, *117*, 62 – 68; c) T. Akita, K. Tanaka, M. Kohyama, M. Haruta, *Surf. Interface Anal.* **2008**, *40*, 1760 – 1763; d) F. Boccuzzi, A. Chiorino, M. Manzoli, P. Lu, T. Akita, S. Ichikawa, M. Haruta, *J. Catal.* **2001**, *202*, 256 – 267; e) M. Daté, M. Okumura, S. Tsubota, M. Haruta, *Angew. Chem.* **2004**, *116*, 2181 – 2184; *Angew. Chem. Int. Ed.* **2004**, *43*, 2129 – 2132; f) N. Shibata, A. Goto, K. Matsunaga, T. Mizoguchi, S. D. Findlay, T. Yamamoto, Y. Ikuhara, *Phys. Rev. Lett.* **2009**, *102*, 4; g) S. Giorgio, S. S. Joao, S. Nitsche, D. Chaudanson, G. Sitja, C. R. Henry, *Ultramicroscopy* **2006**, *106*, 503 – 507.
[4] a) M. I. Buckett, J. Strane, D. E. Luzzi, J. P. Zhang, B. W. Wessels, L. D. Marks, *Ultramicroscopy* **1989**, *29*, 217 – 227; b) M. R. McCartney, P. A. Crozier, J. K. Weiss, D. J. Smith, *Vacuum* **1991**, *42*, 301 – 308; c) M. R. McCartney, D. J. Smith, *Surf. Sci.* **1991**, *250*, 169 – 178.
[5] a) S. Giorgio, M. Cabie, C. R. Henry, *Gold Bull.* **2008**, *41*, 167 – 173; b) Y. Kuwauchi, H. Yoshida, T. Uchiyama, T. Akita, H. Kohno, S. Takeda, *Microsc. Microanal.* **2010**, *16*, 1414; c) T. Tanaka, K. Sano, M. Ando, A. Sumiya, H. Sawada, F. Hosokawa, E. Okunishi, Y. Kondo, K. Takayanagi, *Surf. Sci.* **2010**, *604*, L75 – L78; d) K. Ueda, T. Kawasaki, H. Hasegawa, T. Tanji, M. Ichihashi, *Surf. Interface Anal.* **2008**, *40*, 1725 – 1727.
[6] T. Uchiyama, H. Yoshida, Y. Kuwauchi, S. Ichikawa, S. Shimada, M. Haruta, S. Takeda, *Angew. Chem.* **2011**, *123*, 10339; *Angew. Chem. Int. Ed.* **2011**, *50*, 10157.
[7] a) S. Chenna, R. Banerjee, P. A. Crozier, *Chemcatchem* **2011**, *3*, 1051 – 1059; b) A. Chuvilin, A. N. Khlobystov, D. Obergfell, M. Haluska, S. H. Yang, S. Roth, U. Kaiser, *Angew. Chem.* **2010**, *122*, 197 – 201; *Angew. Chem. Int. Ed.* **2010**, *49*, 193 – 196; c) M.

Koshino, Y. Niimi, E. Nakamura, H. Kataura, T. Okazaki, K. Suenaga, S. Iijima, *Nat. Chem.* **2010**, *2*, 117 – 124; d) M. Koshino, T. Tanaka, N. Solin, K. Suenaga, H. Isobe, E. Nakamura, *Science* **2007**, *316*, 853 – 853; e) E. Nakamura, M. Koshino, T. Saito, Y. Niimi, K. Suenaga, Y. Matsuo, *J. Am. Chem. Soc.* **2011**, *133*, 14151 – 14153.

[8] P. M. Ajayan, L. D. Marks, *Phys. Rev. Lett.* **1989**, *63*, 279 – 282.

[9] a) L. M. Molina, B. Hammer, *Appl. Catal. A* **2005**, *291*, 21 – 31; b) L. M. Molina, B. Hammer, *Phys. Rev. B* **2004**, *69*, 22; c) M. Mavrikakis, P. Stoltze, J. K. Norskov, *Catal. Lett.* **2000**, *64*, 101 – 106.

[10] a) M. Haruta, *Faraday Discuss.* **2011**, *152*, 11 – 32; b) H. Q. Shi, M. Kohyama, S. Tanaka, S. Takeda, *Phys. Rev. B* **2009**, *80*, 155413; c) H. Q. Shi, C. Stampfl, *Phys. Rev. B* **2008**, *77*, 94127.

[11] a) R. F. Egerton, *Electron-Loss Spectroscopy in the Electron Microscope*, 2nd ed., Plenum Pub Corp, New York, **1996**; b) Z. L. Wang, J. Liu, J. M. Cowley, *Surf. Sci.* **1989**, *216*, 528 – 538.

[12] N. Noda, S. Takeda, *Phys. Rev. B* **1996**, *53*, 7197 – 7204.

[13] H. C. Yao, Y. F. Y. Yao, *J. Catal.* **1984**, *86*, 254 – 265.

[14] M. Haruta, S. Tsubota, T. Kobayashi, H. Kageyama, M. J. Genet, B. Delmon, *J. Catal.* **1993**, *144*, 175 – 192.

